

First-principles study of cation distribution in eighteen closed-shell $A^{II}B_2^{III}O_4$ and $A^{IV}B_2^{II}O_4$ spinel oxides

Su-Huai Wei and S. B. Zhang

National Renewable Energy Laboratory, Golden, Colorado 80401

(Received 20 June 2000; published 9 January 2001)

Using a first-principles band-structure method, we have systematically studied the cation distribution in closed-shell $A^{II}B_2^{III}O_4$ and $A^{IV}B_2^{II}O_4$ spinels where the group-II atoms are Mg, Zn, and Cd, the group-III atoms are Al, Ga, and In, and the group-IV atoms are Si, Ge, and Sn. The total energies, the structural parameters, and the band gaps of these compounds in both normal and inverse spinel structures are calculated. Compared with previous model studies, we show that an atomistic method is crucial to correctly identify the stability of the spinels and to calculate the anion displacement parameter u . The preference of cations with delocalized valence d states (e.g., Zn) to form covalent tetrahedral bonds also plays a significant role in determining the cation distribution in the spinels. Furthermore, the electronic structures of these spinel compounds depend strongly on the cation distribution. For most of the spinels studied here, the calculated band gaps for the inverse spinels are smaller than the corresponding normal spinels except for $SnB_2^{II}O_4$.

DOI: 10.1103/PhysRevB.63.045112

PACS number(s): 71.15.Nc, 61.50.Ah, 61.66.Fn

I. INTRODUCTION

Spinel oxides are a group of compounds with the general formula AB_2O_4 . They have the same general crystal structure as the mineral spinel $MgAl_2O_4$. Many of the spinels have interesting electronic and magnetic properties,¹ thus suitable for various technological applications, such as superconductors,^{2,3} magnetic cores,^{4,5} and high-frequency devices.⁵ Since many of the spinels are common minerals, they also have great geophysical interest.⁶⁻⁸ The observation⁹⁻¹² that some of the spinels (e.g., $SnCd_2O_4$, $SnZn_2O_4$, and $CdIn_2O_4$) have large band gaps, and at the same time also have high electroconductivity, make these materials ideal for optoelectronic applications. CdTe solar cells using Cd_2SnO_4/Zn_2SnO_4 as transparent conductor layers have achieved the highest cell efficiency known for this system.¹³ These discoveries have rekindled the interest to study the fundamental physics in these systems.

One of the interesting features for spinels is the wide range of cation distributions found in this system. Some of the spinels (e.g., $MgAl_2O_4$) are known to have the “normal” distribution where $\frac{1}{8}$ of the tetrahedral voids in a face-centered-cubic (fcc) close-packed oxygen sublattice are occupied by the A atoms and $\frac{1}{2}$ of the octahedral voids are occupied by the B atoms (Fig. 1). Other spinels (e.g., $SnZn_2O_4$) are known to have the “inverse” distribution where the tetrahedral voids are occupied by the B atoms and the octahedral voids are occupied by both A and B atoms. Intermediate phases with the formula $(A_{1-x}B_x)[A_xB_{2-x}]O_4$ also exist. Here, cations in the square brackets occupy the octahedral sites and cations in the parentheses occupy the tetrahedral sites. The cation inversion parameter x ranges from 0 for a normal spinel to 1 for an inverse spinel. For a completely random distribution, $x = \frac{2}{3}$. A list of the observed spinel oxides and sulfides, their lattice parameters, and the cation inversion parameters are compiled in Ref. 6. Some of the results are listed in Table I.

Since the observation by Barth and Posnjak¹⁴ that not all spinels have the normal spinel structure, the site preference

problem, namely, what is the stable cation distribution for a specific spinel and why it is so, has attracted significant attention in the last half century.^{4,6,15-21} Most of the previous studies used empirical models of electrostatic energy,^{4,15,22} ligand fields,^{23,24} or the ionic size of the cations^{19,20,25} to explain the cation distributions. Although these models are helpful in providing some basic understanding of the cation distributions in spinels, many exceptions exist that do not obey the “rules” derived from these models. For example, using pseudopotential orbital radii, Burdett, Price, and Price¹⁹ constructed a sorting map to identify the stable cation distributions. They found that $SnCd_2O_4$ falls on the boundary that separates normal spinels from inverse spinels. This suggests that the inverse energy

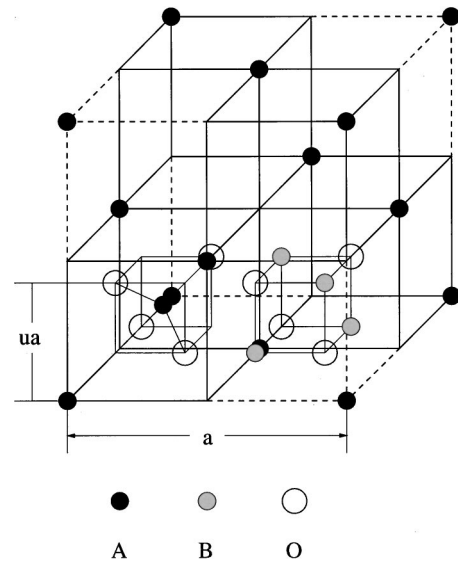


FIG. 1. Crystal structure of normal spinel AB_2O_4 . For clarity, only two octants of the spinel cell are shown. Other octants are occupied alternatively by the tetrahedral (octant without dashed lines) and octahedral clusters (octant with dashed lines) shown in this figure.

TABLE I. Observed structure data for the closed-shell 2-3 and 4-2 spinel oxides studied in this paper. The data are compiled by Hill, Craig, and Gibbs in Ref. 6. For $0 < x < \frac{2}{3}$, the spinel is expected to have a positive inverse energy ΔE and the normal spinel is more stable. For $\frac{2}{3} < x < 1$, the spinel is expected to have a negative ΔE and the inverse spinel is more stable. The temperature associated with the x values in this table is uncertain.

Compound	a (Å)	u	x
2-3 spinels			
MgAl ₂ O ₄	8.0832	0.3874	0.07
MgGa ₂ O ₄	8.2800	0.3790	0.67
MgIn ₂ O ₄	8.8100	0.3820	1.00
ZaAl ₂ O ₄	8.0860	0.3886	0.03
ZnGa ₂ O ₄	8.3300	0.3867	0.00
ZnIn ₂ O ₄			
CdAl ₂ O ₄	8.0780		
CdGa ₂ O ₄	8.5700		0.25
CdIn ₂ O ₄	9.1150	0.3850	1.00
4-2 spinels			
SiMg ₂ O ₄	8.0760		0.00
SiZn ₂ O ₄			
SiCd ₂ O ₄			
GeMg ₂ O ₄	8.2496	0.3758	0.00
GeZn ₂ O ₄			
GeCd ₂ O ₄			
SnMg ₂ O ₄	8.6000	0.3750	1.00
SnZn ₂ O ₄	8.6574	0.3900	1.00
SnCd ₂ O ₄	9.1430	0.3920	1.00

$$\Delta E = E(\text{inverse}) - E(\text{normal}) \quad (1)$$

for SnCd₂O₄ is small. They also found that in the map, CdIn₂O₄ falls in the middle of the inverse spinel region, suggesting that the inverse energy for CdIn₂O₄ is very negative. However, there are strong indication that SnCd₂O₄ is more stable in the inverse structure²⁶ while CdIn₂O₄ is more stable in the normal structure,²⁷ although an early study suggested that CdIn₂O₄ may have the inverse structure.²⁸ Direct experimental determination of the cation distribution in SnCd₂O₄ and CdIn₂O₄ using x-ray diffraction data^{26,27} is rather difficult because the atomic numbers of the cations are similar, thus the diffraction intensity is not sensitive to cation distribution. Furthermore, the virtual crystal approximation (VCA), which neglects the chemical identity of the A and B atoms on a sublattice by assuming averaged type of atom $\langle AB \rangle$, was often used in the early studies to describe the cation distribution in the inverse spinel structure. However, it is not clear whether the VCA is valid for these spinel oxides.

Using a first-principles band structure method within the local density approximation (LDA),²⁹ we systematically studied the site preference of cation distribution in 18 closed-shell $A^{\text{II}}B_2^{\text{III}}O_4$ (2-3) and $A^{\text{IV}}B_2^{\text{II}}O_4$ (4-2) spinels. Here, the group-II atoms are Mg, Zn, and Cd, the group-III atoms are Al, Ga, and In, and the group-IV atoms are Si, Ge, and Sn. Since all the cations considered here have either fully occupied valence d state or no valence d state, the effect of the

ligand field is negligible. We find that the LDA-predicted site preference agrees well with available experimental data. We identify unambiguously that SnCd₂O₄ is more stable in the inverse spinel structure while CdIn₂O₄ is more stable in the normal spinel structure. Compared with previous model studies, we find that (i) the VCA does not predict reliably the cation distribution in spinels. An atomistic method that includes both realistic charge distribution and local atomic relaxations is needed to correctly predict the stability of the spinels. (ii) The anion displacement parameter u depends sensitively on the cation distribution. (iii) The lattice constant has only a weak dependence on the cation distribution. The nearest-neighbor (NN) bond length between the tetrahedral cation and the oxygen atom is about 0.1 Å smaller than the NN bond length between the octahedral cation and the oxygen. (iv) The preference of certain cations to form covalent tetrahedral bonds is a significant factor in determining the cation distribution in spinels. Atoms with shallow occupied d orbitals such as Zn, Cd, Ga, and In prefer to occupy the tetrahedral site rather than the octahedral site. (v) The electronic structures of these spinel compounds depend strongly on the cation distribution. For most of the spinels studied here, the calculated band gaps for the inverse spinels are smaller than the corresponding normal spinels, except for SnB₂^{II}O₄ spinels. In the following, we describe in more detail the spinel crystal structure and our calculation methods and discuss the significant physics of our calculated results.

II. SPINEL CRYSTAL STRUCTURE

A normal AB_2O_4 spinel has a fcc lattice with space group $Fd\bar{3}m$ or O_h^7 . When a fcc cubic cell of edge a and occupied by A atoms is subdivided into eight octants with edge $a/2$ (Fig. 1), four of the octants are occupied by AO_4 clusters and the other four of the octants are occupied by B_4O_4 clusters. The A atom is centered on the AO_4 tetrahedron cluster with four nearest-neighbor O atoms, while the B atom is at the corner of the octahedron cluster with six nearest-neighbor O atoms. The O atoms are positioned in the same way in all octants with one A atom and three B atoms as their nearest neighbors. There are only two structural parameters, the cubic lattice constant a and the anion displacement parameter u . The nearest-neighbor tetrahedral (tetra) bond length R_{tetra} and the nearest-neighbor octahedral (octa) bond length R_{octa} are given by

$$R_{\text{tetra}} = \sqrt{3}(u - 0.25)a,$$

$$R_{\text{octa}} = \sqrt{(u - 0.625)^2 + 2(u - 0.375)^2}a. \quad (2)$$

At $u = 0.3875$, the two bond lengths R_{tetra} and R_{octa} are equal. Furthermore, at $u = 0.375$, when the anions form a perfect fcc sublattice,

$$\partial R_{\text{tetra}} / \partial u = \sqrt{3}a,$$

$$\partial R_{\text{octa}} / \partial u = -a. \quad (3)$$

Thus, when u increases, the tetrahedral bond lengths increase while the octahedral bond lengths decrease, and the tetrahedral bond length increases faster than the octahedral bond length decreases.

In an inverse spinel structure, the tetrahedral sites are occupied by B atoms while the octahedral sites are occupied by equal numbers of A and B atoms. Ideally, to describe the inverse spinel structure one could use a large supercell and occupy the octahedral sites randomly by A and B atoms.³⁰ However, this approach is computationally very expensive. There is, however, a more efficient way to achieve the same result, i.e., using the ‘‘special quasirandom structure’’ (SQS) approach.^{31,32} This approach is based on the fact that the physical properties of an alloy are uniquely determined by its atomic structure, and that the structure can be quantified by the ‘‘atomic correlation functions’’ $\bar{\Pi}_{k,m}$ for atomic clusters (k, m) with k vertices and up to m th neighbor.³³ Hence, if we occupy the octahedral sites in a relatively small unit cell (SQS) by A and B atoms in such a way so that its physically most relevant atomic correlation functions are similar to that for a random occupation, the calculated properties using the SQS will also approach the exact values for the random alloy. The SQS approach has been previously applied to III-V (Refs. 34 and 35) and II-VI (Refs. 36 and 37) zinc-blende alloys as well as to fcc transition-metal alloys.^{38,39} In this study we apply the SQS method for the inverse spinels. We used the same primitive unit cell as for the normal spinel. The structures generated by randomly occupying the four octahedral sites in the unit cell are all crystallographically equivalent. It is interesting to note that this is the same structure observed for some long-range-ordered inverse spinels.⁴

III. METHOD OF CALCULATION

The band-structure and total-energy calculations are performed using the first-principles local density approximation as implemented by the general potential, all electron, relativistic, linearized augmented plane-wave method.⁴⁰ No shape approximations are employed for either the potential or the charge density. We used the Ceperley-Alder exchange correlation potential⁴¹ as parametrized by Perdew and Zunger.⁴² Two special \mathbf{k} points (six equivalent \mathbf{k} points for the inverse structure) in the fcc Brillouin zone are used for the reciprocal space integration. Further increase of the number of \mathbf{k} points changes the total energy difference by less than 0.01 eV. It is well known that LDA underestimate the band gap. Fortunately, however, the LDA errors are mostly canceled when we compare, in this paper, only the band gap differences of crystal structures of the same chemical compounds that differ only in their atomic distributions.

The lattice vectors for both the normal and inverse spinels are kept to be cubic, but all the internal structural parameters are fully relaxed. A recent calculation by Mo and Ching³⁰ for MgAl_2O_4 showed that configuration dependence of physical properties of the inverse spinel is small once the atoms are fully relaxed inside the unit cell. Thus, the error introduced by the use of the finite SQS in our study is expected to be small. The effective u parameters for the inverse spinels are obtained by fitting the averaged tetrahedral bond lengths and

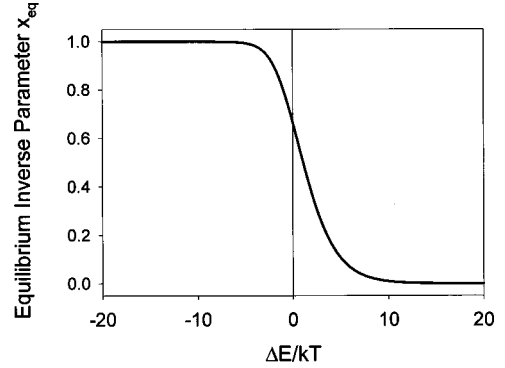


FIG. 2. Calculated equilibrium cation inversion parameter x_{eq} as a function of $\Delta E/kT$ using the model described in the text [Eqs. (4)–(6)].

octahedral bond lengths to Eq. (2).

The total-energy and band-structure calculations are performed at $T=0$. To calculate, at a given temperature T , the equilibrium cation inversion parameter x_{eq} of a spinel $(A_{1-x}B_x)[A_xB_{2-x}]O_4$, we used the model of Navrotsky and Kleppa.¹⁸ In this model, the free energy is

$$\Delta G(x) = \Delta H(x) - T\Delta S(x), \quad (4)$$

where the enthalpy term $\Delta H(x)$ and the entropy term $\Delta S(x)$ is approximated by

$$\Delta H(x) = x\Delta E,$$

$$\Delta S(x) = -k[x \ln x + (1-x)\ln(1-x) + x \ln(x/2) + (2-x)\ln(1-x/2)]. \quad (5)$$

Here, ΔE is the inverse energy of Eq. (1) and k is the Boltzmann constant. In writing Eqs. (4) and (5), we have made the following assumptions: (a) ΔH is a simple linear function of x , (b) the distribution of the cations on each sublattice is random, (c) the nonconfigurational entropy is negligible, and (d) the volume change associated with the cation inversion is negligible. Note that the configuration entropy $\Delta S(x)$ is zero at $x=0$ for the normal spinel. It has a maximum value of $1.91k$ at $x = \frac{2}{3}$ (random cation distribution), and has the value of $1.39k$ at $x=1$ (inverse spinel). The equilibrium cation inversion parameter x_{eq} is the value at which the free energy is minimum. Taking a derivative of $G(x)$ with respect to x and using the expression of Eq. (5), we have

$$x_{\text{eq}} = \frac{\sqrt{9 + 8(c-1)} - 3}{2(c-1)}, \quad (6)$$

where $c = e^{\Delta E/kT}$. Figure 2 depicts the x_{eq} as a function of $\Delta E/kT$. We see that x_{eq} differs significantly from 0 (normal spinel) and 1 (inverse spinel) only if $-5 < \Delta E/kT < 10$.

IV. RESULTS AND DISCUSSIONS

Table II presents our calculated structural parameters a and u for both the normal (N) and inverse (I) spinel structures, the inverse energy ΔE , the equilibrium cation inversion parameter x_{eq} at $T=1200$ K, and the inverse band-gap

TABLE II. Calculated structural parameters a and u for normal (N) and inverse (I) spinels, the inverse energy ΔE , the equilibrium cation inversion parameter x_{eq} at $T=1200$ K, and the inverse band-gap reduction ΔE_g for the 18 closed-shell 2-3 and 4-2 spinel oxides. A positive ΔE indicates that the normal spinel is more stable at low temperature than the inverse spinel. A positive ΔE_g indicates that the normal spinel has a lower band gap than the inverse spinel.

Compound	a_N (Å)	a_I (Å)	u_N	u_I	ΔE (eV/molecule)	x_{eq}	ΔE_g (eV)
2-3 spinels							
MgAl ₂ O ₄	8.072	8.046	0.3887	0.3799	0.50	0.12	-0.66
MgGa ₂ O ₄	8.341	8.283	0.3862	0.3813	-0.05	0.74	-0.80
MgIn ₂ O ₄	8.884	8.846	0.3803	0.3848	-0.06	0.75	-0.55
ZnAl ₂ O ₄	8.073	8.080	0.3895	0.3790	0.92	0.02	-0.77
ZnGa ₂ O ₄	8.311	8.302	0.3863	0.3810	0.48	0.13	-1.43
ZnIn ₂ O ₄	8.868	8.848	0.3803	0.3848	0.26	0.31	-0.94
CdAl ₂ O ₄	8.330	8.360	0.3950	0.3756	1.30	0.00	-0.75
CdGa ₂ O ₄	8.579	8.573	0.3927	0.3776	0.90	0.02	-1.32
CdIn ₂ O ₄	9.130	9.112	0.3873	0.3815	0.54	0.10	-1.07
4-2 spinels							
SiMg ₂ O ₄	8.039	8.106	0.3692	0.3887	0.56	0.09	-0.81
SiZn ₂ O ₄	8.083	8.124	0.3682	0.3882	0.05	0.59	-0.45
SiCd ₂ O ₄	8.617	8.670	0.3612	0.3916	0.74	0.04	-0.81
GeMg ₂ O ₄	8.266	8.338	0.3762	0.3567	0.20	0.38	0.03
GeZn ₂ O ₄	8.325	8.360	0.3756	0.3861	-0.36	0.97	-0.06
GeCd ₂ O ₄	8.851	8.895	0.3682	0.3899	-0.05	0.74	-0.32
SnMg ₂ O ₄	8.566	8.642	0.3833	0.3835	-0.17	0.87	0.81
SnZn ₂ O ₄	8.631	8.658	0.3830	0.3833	-0.64	1.00	0.60
SnCd ₂ O ₄	9.134	9.164	0.3760	0.3873	-0.71	1.00	0.14

reduction ΔE_g for the 18 compounds. Table III lists our calculated tetrahedral and octahedral cation-oxygen nearest-neighbor bond lengths. In this paper, we do not consider the possible existence of other structures that, for some of these compounds, may have lower total energy than the spinels.^{26,43,44}

A. Comparison with experiment

Comparing the calculated results in Table II and the experimental data⁶ in Table I we find the following results.

TABLE III. Calculated tetrahedral (tetra) and octahedral (octa) nearest-neighbor cation-O bond lengths for the cations studied in this paper. Results are averaged over different spinel compounds and the standard deviations are also given.

Bond	R_{tetra}	R_{octa}
Mg-O	1.96±0.02	2.05±0.03
Zn-O	1.97±0.02	2.07±0.03
Cd-O	2.14±0.03	2.24±0.03
Al-O	1.82±0.02	1.93±0.02
Ga-O	1.89±0.02	2.00±0.02
In-O	2.07±0.02	2.16±0.02
Si-O	1.66±0.02	1.83±0.02
Ge-O	1.81±0.02	1.94±0.02
Sn-O	1.99±0.02	2.08±0.02

(i) The calculated lattice constants are within 1% of the experimental values, except for CdAl₂O₄. Since the cited experimental value^{6,17} of 8.078 Å for CdAl₂O₄ is smaller than the one for ZnAl₂O₄ (8.086 Å), while the atomic size of Cd is much larger than Zn, we believe that the cited experimental value is possibly incorrect.

(ii) The calculated anion displacement parameter u depends sensitively on the cation distribution. For example, at normal spinel structure, the u parameters for ZnAl₂O₄ and SnCd₂O₄ are 0.3895 and 0.3760, respectively, while at inverse spinel structure the effective u parameters are 0.3790 and 0.3873, respectively. If we use the measured or calculated cation inversion parameter x and assume the u parameter varies linearly with x , the calculated u are in good agreement with experimental data,⁶ considering the fact that the uncertainties in the measured u parameter and the inversion parameter x are relatively large. We notice that the discrepancy between the calculated values and the measured values for the Sn compounds is somewhat larger than the other compounds.

(iii) The calculated cation inversion energy ΔE for most of the 2-3 spinels are positive, i.e., they are more stable in the normal spinel structure, except for MgGa₂O₄ and MgIn₂O₄, which are slightly negative, thus, more stable in the inverse spinel structure. For 4-2 spinels, all the Si spinels and GeMg₂O₄ are more stable in the normal spinel structure, while the other 4-2 spinels are more stable in the inverse spinel structure. These results are consistent with experimen-

tal observations⁶ except for CdIn₂O₄. Our calculated $\Delta E = 0.54$ eV/molecule for CdIn₂O₄ is strongly positive, suggesting that it should have a normal spinel structure. An early experiment by Skribljak, Dasgupta, and Biswas²⁸ concluded that it was probably inverse. However, more recent estimates of Shannon, Gillson, and Bouchard²⁷ concluded that it was probably a normal spinel. The difficulty in identifying the crystal structure of CdIn₂O₄ experimentally is due to the fact that the atomic numbers of Cd and In differ only by 1, thus the x-ray diffraction intensities of normal and inverse CdIn₂O₄ spinels are very similar.

(iv) By measuring experimentally the inverse parameter x as a function of temperature, one can invert Eq. (6) to estimate the inverse energy ΔE . Using this approach, the experimentally estimated inverse energy ΔE for the mineral spinel MgAl₂O₄ is 0.48 eV,⁴⁵ which can be compared with the calorimetry date of 0.39 ± 0.09 eV.¹⁸ The experimentally estimated value for MgGa₂O₄ is $\Delta E = -0.11$ eV.⁴⁵ These values are in good agreement with our calculated values of 0.50 and -0.05 eV, respectively, for MgAl₂O₄ and MgGa₂O₄.

B. Analysis of the general trends

From our systematic studies we observe the following trends.

(i) In Table III, we see that the cation-O bond lengths, and thus, the ionic atomic sizes of the cations in the same group, increase as the cation atomic number increases. That is, the atomic size increases from Mg to Zn to Cd, from Al to Ga to In, and from Si to Ge to Sn. It is interesting to note that in the more covalent zinc-blende compounds (e.g., MgSe, ZnSe, AlAs, and GaAs) Mg-anion bond lengths are larger than Zn-anion bond lengths, and Al-anion bond lengths are larger than Ga-anion bond lengths.⁴⁶ In Ref. 19, the pseudopotential orbital radii used by Burdett, Price, and Price have $r(\text{Mg}) > r(\text{Zn})$, which is not consistent with the ionic radii derived here.

(ii) The ionic atomic size decreases as the atomic valence increases, i.e., it decreases from Mg to Al to Si, from Zn to Ga to Ge, and from Cd to In to Sn. This is because for cations with higher valence, the net charges of the ionic cores are larger after removing the valence electrons. Therefore, cations with higher valence are more tightly bound to the nucleus and thus have a smaller ionic radius.

(iii) The octahedral cation-O bond length is ~ 0.1 Å larger than the tetrahedral bond length. This is because the octahedral site is more open than the tetrahedral site. Our results agree reasonably well with the empirical results of Shannon²⁵ and that of O'Neill and Navrotsky.²⁰ However, our results do not agree with Mo and Ching's results³⁰ who find a much larger difference of 0.5 Å in MgAl₂O₄.

(iv) For 2-3 spinels, the calculated lattice constant for the normal spinel structure is generally slightly larger than the one for the inverse spinel structure. For 4-2 spinels, the opposite is true, i.e., the lattice constant for the normal spinel is always smaller than the one for inverse spinel. This is because when a larger group-II atom (e.g., Cd in SnCd₂O₄ or Mg in MgAl₂O₄) occupies the tight tetrahedral site, the lattice constant tends to expand a little to accommodate the

larger atom, despite the fact that most of the changes are accommodated by the displacement of the anions and the ensuing change of the parameter u .

(v) u_N for 2-3 spinels (~ 0.387) are larger than u_N for 4-2 spinels (~ 0.373). This is because the A^{II} -O tetrahedral bond lengths are similar to the B^{III} -O octahedral bond lengths for 2-3 spinels (Table III). Thus, the O atom will displace from its ideal position at $u = 0.375$ towards the position $u = 0.3875$ where the tetrahedral bond length and the octahedral bond length are equal. On the other hand, for 4-2 spinels, the A^{IV} -O tetrahedral bond length is much smaller than the B^{II} -O octahedral bond length (Table III). Therefore, the average u_N is close to the ideal value of $u = 0.375$, where the ratio between the tetrahedral bond length and the octahedral bond length is $\sqrt{3}/2$.

(vi) For 2-3 spinels, compounds with large A^{II} atoms, and thus large u_N (e.g., CdB₂O₄) tend to have the normal spinel structure (i.e., large positive ΔE). For 4-2 spinels, the situation is reversed. Compounds with large A^{IV} atoms (e.g., SnB₂O₄) tend to have the inverse spinel structure (i.e., large negative ΔE).

(vii) For compounds with similar structural parameters, e.g., MgB₂^{III}O₄ and ZnB₂^{III}O₄, the inverse energy ΔE for ZnB₂^{III}O₄ is much larger than for MgB₂^{III}O₄. This indicates that Zn, which has shallow occupied valence d states, prefers to occupy the tetrahedral site. Similar situations exist in 2-3 Al and Ga spinels, and in 4-2 Mg and Zn spinels. We find that Zn and Ga have a stronger preference to occupy the tetrahedral site. In general, atoms with shallow occupied valence d states (Zn, Cd, Ga, and In) prefer to occupy the tetrahedral site.

C. Electrostatic energy

To understand the general trends discussed above, especially trend (vi), we have studied the electrostatic energy for these spinels and compared with previous models.^{15,22,47} The electrostatic energy has long been considered to be one of the most important factors in determining the cation distribution in spinels, especially for the closed shell spinels studied here. Verwey and Heilmann¹⁵ performed the first calculation of the electrostatic energy

$$E_M = -M(e^2/a), \quad (7)$$

of normal and inverse spinels as a function of u . Here, M is the Madelung constant. A large Madelung constant means a lower electrostatic energy. Verwey and Heilmann used nominal charges ($Q = 2, 3, 4$, and -2 for group-II, -III, -IV, and O atoms, respectively) and the VCA to describe the inverse structure. They concluded from their electrostatic energy calculation that all 2-3 spinels should be stable in the normal arrangement, while all 4-2 spinels should be stable in the inverse arrangement. This "rule" clearly does not agree with the experimental observation of Table I or the theoretical calculations of Table II. Latter calculations by Hermans, Weenk, and Van Gool,⁴⁷ and by Thompson and Grimes²² revealed some numerical error in the earlier work.¹⁵ They show that for 2-3 spinels, normal distribution is favored if $u > 0.3805$, while for 4-2 spinels inverse distribution is fa-

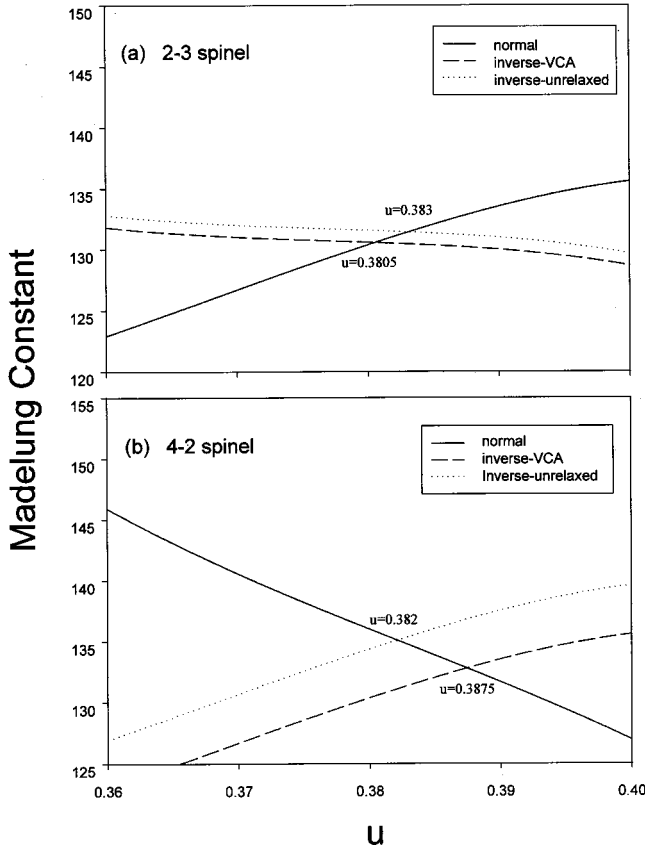


FIG. 3. Calculated Madelung constants [Eq. (7)] as a function of the anion displacement u for the normal (solid line) and inverse spinels for (a) 2-3 spinels and (b) 4-2 spinels. The inverse spinels are calculated with (dashed line) or without (dotted line) the VCA charge distribution. The VCA atomic positions are used in both calculations.

vored if $u > 0.3875$. The calculated Madelung constants are plotted in Fig. 3. We find from Fig. 3 that the Coulomb energy^{47,22} explains qualitatively trend (vi) above. For example, for the 2-3 normal spinel, the Madelung constant increases with u , while for the 2-3 inverse spinel the Madelung constant decreases with u [Fig. 3(a)]. For the 4-2 spinel, the trend is reversed [Fig. 3(b)]. The electrostatic model thus explains why the 2-3 spinel with a large u prefers the normal structure, while the 4-2 spinel with a large u prefers the inverse structure.

However, this simple electrostatic model cannot be used to predict the inverse energy quantitatively for the following reasons: First, nominal charges are used, while in reality the charge on each atom is screened and depends on the local environment.⁴⁸ Second, the VCA is used to describe the charge distribution in the inverse spinel structure. To see the effect of the VCA charge distribution, we have calculated the Madelung constant using the actual nominal ionic charge on each site instead of the averaged one. In this calculation, we keep the atoms at their VCA positions. Figure 3 compares the calculated Madelung constants. We find that the VCA always underestimates the Madelung constant. The error is proportional to $(Q_A - Q_B)^2$. Therefore, the error is four times larger in 4-2 spinels than in 2-3 spinels. When the

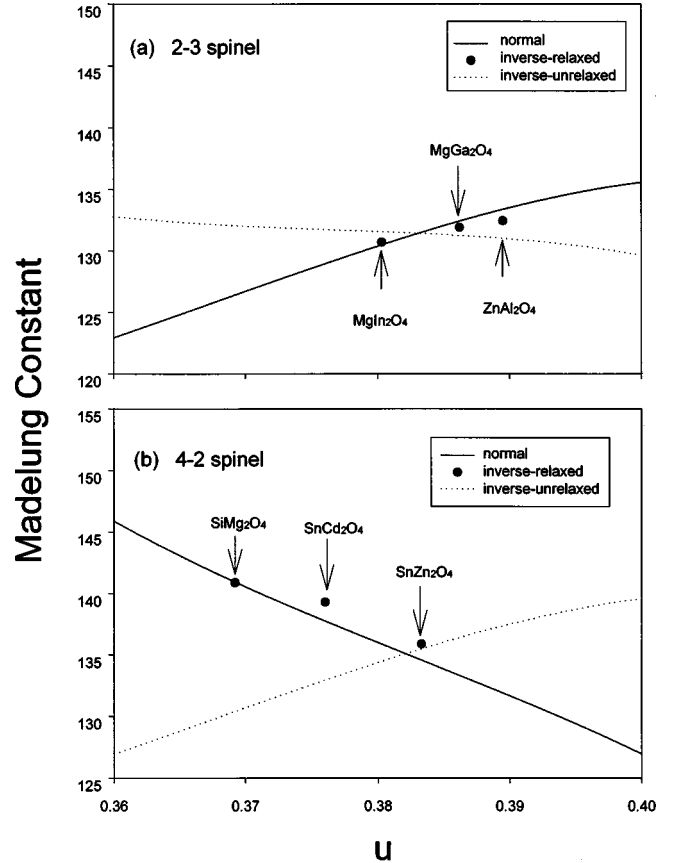


FIG. 4. Similar to Fig. 3. The solid dots are the results calculated for MgGa_2O_4 , MgIn_2O_4 , ZnAl_2O_4 , SiMg_2O_4 , SnZn_2O_4 , and SnCd_2O_4 using the LDA calculated, fully relaxed atomic positions.

correct ionic charge is taken into account, the critical u value at which the Madelung constants for the normal and inverse spinels are equal is shifted from $u = 0.3805$ to $u \sim 0.383$ for 2-3 spinels and from $u = 0.3875$ to $u \sim 0.382$ for 4-2 spinels. Third, the electrostatic model assumes implicitly that the effective u parameters for the normal and inverse spinels are the same and that cations are at their ideal positions. We find that, in most cases, this assumption is not valid. For some of the spinels (e.g., ZnAl_2O_4 and SnCd_2O_4) the u parameters for the normal and inverse spinels are very different. If we use the u parameters for the normal structure, we would expect from the electrostatic model that both ZnAl_2O_4 ($u_N = 0.3895$) and SnCd_2O_4 ($u_N = 0.3760$) would have the normal spinel structure (Figs. 3 and 4). However, if we use the u parameters for the inverse structure, we would expect from the electrostatic model that both ZnAl_2O_4 ($u_I = 0.3790$) and SnCd_2O_4 ($u_I = 0.3873$) would have the inverse spinel structure (Fig. 3). This analysis indicates that one cannot judge *a priori* the stability of spinels from a single u parameter.

Figure 4 shows the effect of atomic relaxation on the Madelung constants for some of the spinels. For each compound, the Madelung constant is calculated at three configurations: (a) at the normal spinel structure, (b) at the inverse unrelaxed structure, and (c) at the fully relaxed inverse atomic position (solid dots). The arrows in Fig. 4 point to the u parameters associated with each compound at the normal

spinel structure. For the inverse unrelaxed structure, atoms are switched but no further atomic relaxation from the normal spinel positions is allowed. That is, the inverse spinel is assumed to have the same u parameter as the normal spinel. Our calculated results are used for the fully relaxed inverse spinel atomic positions. For the 4-2 spinels with large cation size mismatch (e.g., SiMg_2O_4 and SnCd_2O_4 , reflected by their large differences between the u parameters for the normal and inverse structure in Table II), the effects of atomic relaxation on electrostatic energy are very large. SnCd_2O_4 has a large Madelung constant in the inverse spinel structure only after the atomic relaxation. The relaxation effect is negligible for SnZn_2O_4 , because Zn and Sn have very similar atomic size (Table III), which is also reflected by its nearly identical u parameters for normal ($u=0.3830$) and inverse ($u=0.3833$) structures. The relaxation effects for the 2-3 spinels are also relatively small because the charge differences between the cations are smaller in 2-3 spinels than in 4-2 spinels. In both cases, we find that the electrostatic energy differences between normal and inverse spinels become much smaller after atomic relaxation.

D. Change of the band gap

To see how the cation distribution affects the electronic structure of a spinel, we have calculated the difference of the direct band gap at the zone center (Γ) between normal and inverse spinels.

$$\Delta E_g = E_g(\text{inverse}) - E_g(\text{normal}). \quad (8)$$

The results are given in the last column of Table II. We find that for most of the spinels studied here, the calculated band gaps for the inverse spinels are smaller than those of the normal spinels, i.e., ΔE_g is negative. This can be understood by noticing that in the inverse structure, the local symmetry is reduced by the distribution of atoms and atomic relaxations. This lowering of local symmetry causes further level repulsion within the valence band and within the conduction band, pushing up the valence-band maximum and pushing down the conduction-band minimum states, thus lowering the band gap. This effect is similar to that observed in semiconductor alloys, where due to symmetry-lowering-induced band repulsion, the alloy band gap is smaller than the com-

position averaged band gap.³² However, for $\text{SnB}_2^{\text{II}}\text{O}_4$ (also for GeMg_2O_4), due to the small change in the anion displacement u as well as the charge transfer from Sn to group-II cations in forming the inverse structure (the Sn 5s orbital energy is about 5 eV lower than the group-II cations), the band gap for the inverse structure is *larger* than the one for the normal structure. The effect of the cation distribution on the change of the band gap can be large. For example, $\Delta E_g = -1.32$ eV for CdGa_2O_4 and $\Delta E_g = 0.81$ eV for SnMg_2O_4 . Thus, in principle, one can control the band gap by controlling the cation inversion parameter x . This provides an opportunity for band-gap engineering of these materials for specific technological applications.

V. SUMMARY

Using a first-principles band-structure method, we have systematically studied the cation distribution in closed-shell $A^{\text{II}}B_2^{\text{III}}\text{O}_4$ and $A^{\text{IV}}B_2^{\text{II}}\text{O}_4$ spinels. Our predicted site preference agrees very well with available experimental data. We identify unambiguously that SnCd_2O_4 is more stable in the inverse spinel structure, while CdIn_2O_4 is more stable in the normal spinel structure. Compared with previous model studies, we find that (i) an atomistic method that includes both realistic charge distribution and atomic relaxations is needed to correctly predict the cation distribution in these spinels. (ii) The anion displacement parameter u depends sensitively on the cation distribution. (iii) The preference of some of the cations to form covalent tetrahedral bonds is a significant factor contribution in determining the cation distribution of the spinels. Atoms with shallow valence d states such as Zn and Ga as well as Cd and In prefer to occupy the tetrahedral site rather than the octahedral site. Our predicted changes in the band gaps as function of the cation distribution provides a basis for band-gap engineering of these materials for specific technological applications.

ACKNOWLEDGMENTS

We thank T. J. Coutts and D. L. Young for helpful discussions and Gus Hart for careful reading of our manuscript. This work was supported by U.S. Department of Energy, Grant No. DE-AC36-98-GO10337.

¹F. S. Galasso, *Structure and Properties of Inorganic Solids* (Pergamon, New York, 1970).

²D. C. Johnston, H. Prakash, W. H. Zachariasen, and R. Viswanathan, *Mater. Res. Bull.* **8**, 777 (1973).

³R. W. McCallum, D. C. Johnston, C. A. Luengo, and M. B. Maples, *J. Low Temp. Phys.* **25**, 177 (1976).

⁴E. W. Gorter, *Philips Res. Rep.* **9**, 295 (1954).

⁵R. E. Vandenberghe and E. DeGrave in *Mössbauer Spectroscopy Applied to Inorganic Chemistry*, edited by G. J. Long and F. Grandjean (Plenum, New York, 1989), Vol. 3, p. 59.

⁶R. J. Hill, J. R. Craig, and G. V. Gibbs, *Phys. Chem. Miner.* **4**, 317 (1979).

⁷D. L. Anderson, *Science* **223**, 347 (1984).

⁸Y.-M. Chiang and W. D. Kingery, *J. Am. Ceram. Soc.* **72**, 271 (1989); **73**, 1153 (1990).

⁹A. J. Nozik, *Phys. Rev. B* **6**, 453 (1972).

¹⁰M. Labeau, V. Reboux, D. Dhahri, and J. C. Joubert, *Thin Solid Films* **136**, 257 (1986).

¹¹N. Ueda, T. Omata, N. Hikuma, K. Ueda, H. Mizoquchi, T. Hashimoto, and H. Kawazoe, *Appl. Phys. Lett.* **61**, 1954 (1992).

¹²T. J. Coutts, X. Wu, W. P. Mulligan, and J. M. Webb, *J. Electron. Mater.* **25**, 935 (1996).

¹³X. Z. Wu, R. Ribelin, R. G. Dhere, D. S. Albin, T. A. Gessert, S. Asher, D. H. Levi, A. Mason, H. R. Moutinho, and P. Sheldon,

- in *Proceedings of 28th IEEE PVSC* edited by J. Benner (IEEE, New York, in press).
- ¹⁴T. F. W. Barth and E. Posnjak, *Z. Kristallogr.* **82**, 325 (1932).
- ¹⁵E. J. W. Verwey and E. L. Heilmann, *J. Chem. Phys.* **15**, 174 (1947).
- ¹⁶A. Miller, *J. Appl. Phys.* **30**, 245 (1959).
- ¹⁷R. W. G. Wyckoff, *Crystal Structures* (Interscience, New York, 1965), 2nd ed., Vol. 3.
- ¹⁸A. Navrotsky and O. J. Kleppa, *J. Inorg. Nucl. Chem.* **29**, 2701 (1967).
- ¹⁹J. K. Burdett, G. D. Price, and S. L. Price, *J. Am. Chem. Soc.* **104**, 92 (1982).
- ²⁰H. St. C. O'Neill and A. Navrotsky, *Am. Mineral.* **68**, 181 (1983).
- ²¹A. N. Cormack, G. V. Lewis, S. C. Parker, and C. R. A. Catlow, *J. Phys. Chem. Solids* **49**, 53 (1988).
- ²²P. Thompson and N. W. Grimes, *Philos. Mag.* **36**, 501 (1977).
- ²³J. D. Dunitz and L. E. Orgel, *J. Phys. Chem. Solids* **3**, 318 (1957).
- ²⁴D. S. McClure, *J. Phys. Chem. Solids* **3**, 311 (1957).
- ²⁵R. D. Shannon, *Acta Crystallogr., Sect. A: Cryst. Phys., Diffr., Theor. Gen. Crystallogr.* **32**, 751 (1976).
- ²⁶L. A. Siegel, *J. Appl. Crystallogr.* **11**, 284 (1978).
- ²⁷R. D. Shannon, J. L. Gillson, and R. J. Bouchard, *J. Phys. Chem. Solids* **38**, 877 (1977).
- ²⁸M. Skribljak, S. Dasgupta, and A. B. Biswas, *Acta Crystallogr.* **12**, 1049 (1959).
- ²⁹P. Hohenberg and W. Kohn, *Phys. Rev.* **136**, B864 (1964); W. Kohn and L. J. Sham, *ibid.* **140**, A1133 (1965).
- ³⁰S.-D. Mo and W. Y. Ching, *Phys. Rev. B* **54**, 16 555 (1996).
- ³¹A. Zunger, S.-H. Wei, L. G. Ferreira, and J. E. Bernard, *Phys. Rev. Lett.* **65**, 353 (1990).
- ³²S.-H. Wei, L. G. Ferreira, J. E. Bernard, and A. Zunger *Phys. Rev. B* **42**, 9622 (1990).
- ³³J. M. Sanchez, F. Ducastelle, and D. Gratias, *Physica (Amsterdam)* **182A**, 334 (1984).
- ³⁴K. A. Mader and A. Zunger, *Appl. Phys. Lett.* **64**, 2882 (1994).
- ³⁵J. S. Nelson, L. R. Dawson, C. Y. Fong, and L. A. Hemstreet, *Superlattices Microstruct.* **23**, 1053 (1998).
- ³⁶S.-H. Wei and A. Zunger, *Phys. Rev. B* **43**, 1662 (1991); **43**, 14 272 (1991).
- ³⁷A. M. Saitta, S. de Gironcoli, and S. Baroni, *Phys. Rev. Lett.* **80**, 4939 (1998).
- ³⁸Z. W. Lu, S.-H. Wei, and A. Zunger, *Phys. Rev. B* **44**, 10 470 (1991).
- ³⁹Z. W. Lu, S.-H. Wei, and A. Zunger, *Phys. Rev. B* **45**, 10 314 (1992).
- ⁴⁰S.-H. Wei and H. Krakauer, *Phys. Rev. Lett.* **55**, 1200 (1985), and references therein.
- ⁴¹D. M. Ceperly and B. J. Alder, *Phys. Rev. Lett.* **45**, 566 (1980).
- ⁴²J. P. Perdew and A. Zunger, *Phys. Rev. B* **23**, 5048 (1981).
- ⁴³M. Tromel, *Z. Anorg. Allg. Chem.* **371**, 237 (1969).
- ⁴⁴M. E. Bowden and C. M. Cardile, *Powder Diffr.* **5**, 36 (1990).
- ⁴⁵E. Stoll, *J. Phys. (France)* **25**, 447 (1964).
- ⁴⁶*Numerical Data and Functional Relationships in Science and Technology*, edited by O. Madelung, M. Schulz, and H. Weiss, Landolt-Bornstein, New Series Group III, Pts. A and B, Vol. 17 (Springer-Verlag, Berlin, 1982).
- ⁴⁷L. Hermans, J. Weenk, and W. Van Gool, *Zeitschrift für Physikalische Chemie, Neue Folge* **88**, 15 (1974).
- ⁴⁸R. Magri, S.-H. Wei, and A. Zunger, *Phys. Rev. B* **42**, 11 388 (1990).